



## Low Order Modelling of Direct and Indirect Combustion Noise Contributions in a Gas Turbine Model Combustor

Mahmoudi, Y., Dowling, A., & Swaminathan, N. (2017). Low Order Modelling of Direct and Indirect Combustion Noise Contributions in a Gas Turbine Model Combustor. In 24th International Congress on Sound and Vibration (ICSV24).

### Published in:

24th International Congress on Sound and Vibration (ICSV24)

### Queen's University Belfast - Research Portal:

[Link to publication record in Queen's University Belfast Research Portal](#)

### General rights

Copyright for the publications made accessible via the Queen's University Belfast Research Portal is retained by the author(s) and / or other copyright owners and it is a condition of accessing these publications that users recognise and abide by the legal requirements associated with these rights.

### Take down policy

The Research Portal is Queen's institutional repository that provides access to Queen's research output. Every effort has been made to ensure that content in the Research Portal does not infringe any person's rights, or applicable UK laws. If you discover content in the Research Portal that you believe breaches copyright or violates any law, please contact [openaccess@qub.ac.uk](mailto:openaccess@qub.ac.uk).

# LOW ORDER MODELLING OF DIRECT AND INDIRECT COMBUSTION NOISE CONTRIBUTIONS IN A GAS TURBINE MODEL COMBUSTOR

Yasser Mahmoudi

*Queen's University of Belfast, Belfast, BT9 5AH, UK  
email: s.mahmoudilarimi@qub.ac.uk*

Ann Dowling, Nedunchezian Swaminathan

*University of Cambridge, Cambridge, CB2 1PZ, UK*

The present work deals with a low order modelling of the differentiation of combustion noise sources for a generic premixed and pressurized combustor at École Centrale Paris. The contributions of direct and indirect noise to the unsteady pressure within the combustor are obtained. The LOTAN (Low-Order Thermo-Acoustic Network model) code is used to obtain Green's function. LOTAN determines the linear acoustic, entropic and vortical waves due to a harmonic variation in the heat release rate. We studied the effect of different upstream boundary conditions on the prediction of Green's function. To predict the combustion noise, the Green's functions are combined with the spectrum of heat release rate fluctuation that is obtained by post-processing the compressible LES data as well as utilising the spectral model. The combustion noise source for this spectral model depends on the mean flow and turbulence statistics which are found from RANS calculations. Results show that the sound calculated using two approaches are in good agreement with the measured data. It is seen that at some frequencies the indirect entropy noise is comparable to direct acoustic noise within the combustor. While previous high fidelity LES and experimental studies on this combustor have concluded that indirect entropy noise has negligible role in the generation of the total noise in the combustor. This is because these studies could not discriminate fully between the direct and indirect noise elements: their analysis includes the multiple reflection of entropy-generated noise by the combustor boundaries as direct acoustic noise.

Keywords: combustion noise, direct and indirect noise, low order modelling

---

## 1. Introduction

The implementation of advanced low-noise aircraft engine technologies made noise contributions from gas turbine combustors increasingly important. This is partially because advances in design have reduced the other noise sources, and partially because next generation combustion modes burn more unsteadily [1]. The broadband combustion noise radiated by a combustor comprises two components 'direct' and 'indirect'. Fluctuation in heat release from the turbulent flame generates acoustic waves which constitutes the 'direct' combustion noise. The 'indirect' combustion noise is generated when entropy fluctuations or vorticity perturbations is accelerated through the downstream nozzle located at the downstream outlet of a combustor [2]. In the experiment it is very challenging to differentiate the contributions of direct and indirect noise sources in the production of total noise generated in a combustor. This requires development of a reliable prediction tools. In this regard, the capability of high fidelity prediction tools based on large eddy simulations (LES) and hybrid CFD/CAA-methods (computational fluid dynamics/computational aeroacoustics) were

demonstrated for enhancing the understanding of the physical processes involve in the generation of combustion noise in laboratory scale as well as full scale engines [3, 4] . Nonetheless, in addition to demanding high computational costs, these techniques were not capable of differentiating the contributions of direct and indirect combustion noise. Analytical models introduce simplifications with respect to the geometry and flow field which limit their validity to simple cases. Therefore, for complex cases different components of the geometries are represented by series of analytical elements which are linked through network models [5], the so-called low-order models. These tools provide the fastest approach for the prediction of the combustion noise in the combustors under various operating conditions and also capable of differentiating the contribution of direct and indirect combustion noise [1, 6, 7]. To meet this requirement, the present work deals with a low order modelling of the differentiation of combustion noise sources for a generic premixed and pressurized combustor (CESAM-HP combustor) at École Centrale Paris. The LOTAN (Low-Order Thermo-Acoustic Network model) code (e.g. [6-9]) is used to obtain Green’s function (transfer function), which determines the linear acoustic, entropic and vortical waves due to a harmonic variation in the heat release rate. Then, in order to predict the combustion noise, this Green’s function is combined with the spectrum of heat release rate fluctuation that is the source for combustion noise. To obtain this spectrum two approaches are utilised. For the first approach, the high fidelity compressible LES data is post-processed [10]. The second approach is based on the spectral model developed by Hirsch et al. [11] and recently extended by Liu et al. [12]. This approach utilizes the turbulence quantities of the RANS to compute the heat release spectrum [12]. In a recent work by Ulrich et al. [5] is it demonstrated the capability of LOTAN code in combination with the spectral in predicting the total combustion noise in the CESAM-HP combustor.

## 2. CESAM-HP combustor rig

The details of the CNRS rig is given in [13] as shown schematically in Fig. 1. The CESAM-HP test rig represents a rectangular combustion chamber with length 0.14 m, which is connected with the atmosphere via a convergent-divergent nozzle (with length of 0.219 m) mounted at the downstream end of the combustor. A straight duct with length of 0.1345m and a swirler are installed at the upstream side in order to inject the mixture of propane and air.

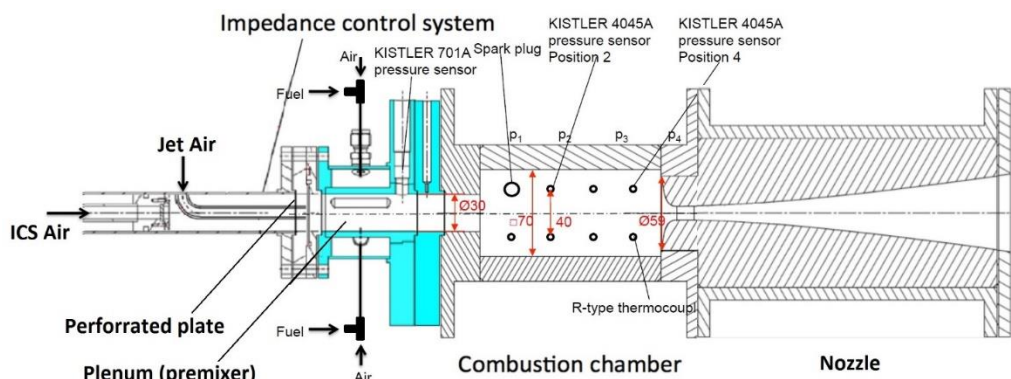


Figure 1: Schematic of CNRS combustor rig [13].

Depending on the operating point additional pure air is injected through a perforated screen. An Impedance Control System (ICS), which consists of a perforated plate backed by a cavity of variable depth is used to provide an axial flow in order to prevent flame flashback as well as to control the acoustic impedance [13]. Air and propane mixture is then admitted tangentially into the plenum. This creates a swirling motion that increases stability during lean combustion operation and creates a more compact flame. Then, the premixed mixture enters the combustion chamber with a swirling motion and is ignited with a spark plug. Thermocouples and pressure sensors are mounted at four potential positions. The exhaust nozzle is also deployed to accelerate the flow of burnt gases and increase the mean pressure in the combustion chamber. This condition is necessary to generate indi-

rect noise from entropy fluctuations generated by the turbulent flame. The nozzle is then open to the atmosphere at its end. In the experiment three different operating points are defined by variations of the air mass flow rates through the swirler, perforated screen and axial jet inlet. The chamber is operated under lean conditions with fixed global equivalence ratio of 0.85 each time. In the present study only one out of three operating points is investigated, which is referred here to as OP-13-5-0 given in Table 1. This operating point features the most stable combustion conditions.

Table 1: Operating condition of the combustor [13] examined in this work.

Swirler mass flow	13 g/s (air) + 0.983 g/s (fuel)
Axial air of impedance control system (ICS) mass flow	0
Axial air jet mass flow	5 g/s
Equivalence ratio	0.85
Total temperature inlet	296.5 K
Mean static pressure	2.3 bar

### 3. Description of the model

#### 3.1 Combustion noise spectrum

In this section we first summarise the relationship between the spectrum of heat release rate fluctuations and the spectrum of the pressure perturbations. The pressure perturbation  $\hat{p}(\vec{x}, \omega)$  generated by unsteady heat per unit volume  $\hat{q}(\vec{y}, \omega)$  can be obtained as

$$\hat{p}(\vec{x}, \omega) = \int_{v_f} \hat{G}_1(\vec{y}, \vec{x}, \omega) \hat{q}(\vec{y}, \omega) d^3 \vec{y}, \quad (1)$$

where  $\omega$  is the angular frequency,  $v_f$  denotes the volume of the flame brush and the prime denotes a perturbation from the mean.  $\hat{G}_1$  is the Green's function that represents the pressure generated at  $(\vec{x}, \omega)$  due to an impulse of rate of heat addition. This function is the pressure solution of linearized Euler equations in the combustor that satisfies the appropriate inlet and outlet boundary conditions. In a similar way the entropy fluctuations can be obtained as a volume integral of the product of a different Green function  $\hat{G}_2$  with the rate of heat release/unit volume. We use the LOTAN network model to obtain these Green's functions  $\hat{G}_1$  and  $\hat{G}_2$ . The power spectral density,  $\hat{P}(\vec{x}, \omega)$  is a statistical quantity measurable in experiments and defined as

$$\hat{P}(\vec{x}, \omega) = \int_{v_f} \left| \hat{G}_1(\vec{y}, \vec{x}, \omega) \right|^2 \psi_q(\vec{y}, \omega) V_{\text{cor}} d^3 \vec{y}. \quad (2)$$

In Eq. (2)  $\psi_q$  is the cross-power spectral density of heat release fluctuations and correlation volume of the fluctuating heat release rate is  $V_{\text{cor}}$ . The sound pressure level (SPL) is hence characterized by  $\hat{P}(\vec{x}, \omega)$  as  $10 \log_{10}(\hat{P} / p_{\text{ref}}^2)$ , where the reference acoustic pressure is  $p_{\text{ref}} = 2 \times 10^{-5} \text{ pa}$ .

When the heat release is so concentrated that  $\hat{G}_1(\vec{y}, \vec{x}, \omega)$  varies little over the combustion zone,  $\hat{G}_1(\vec{y}, \vec{x}, \omega)$  can be taken outside the source integral with respect to source position in Eq. (2) and then LOTAN needs to be run only once for each mode number and frequency. In Eq. (2) the product of heat release rate spectrum  $\psi_q(\vec{y}, \omega)$  and its correlation volume needs to be integrated over the flame brush. This is equivalent to integrating the contributions from the coherent sources of combustion noise with a correlation volume  $V_{\text{cor}}$  over the flame volume. For this purpose we utilised the spectral model of Hirsch et al. [11] and modified by Liu et al. [12]. The spectrum of the heat release rate fluctuation can also be obtained using the LES simulation of the turbulent flame. Thus, we post-processed the results of compressible LES of CESAM-HP combustor [13] to predict the inte-

gral of heat release spectrum over the flame brush and the results are compared with that obtained using the spectral model.

### 3.2 Green's function calculation using LOTAN

The Green's function determines the linear acoustic, entropic and vortical waves due to a harmonic variation in the heat release rate. We calculate its Fourier transform  $\hat{G}(\vec{y}, \vec{x}, \omega)$  using a network model called LOTAN (e.g. [6, 7, 9]). In LOTAN the geometry is modelled by a network of modules describing its features, such as straight ducts, area changes and heating zones. In straight duct sections, the model neglects variation with radius, and assumes a uniform axial mean flow and either one-dimensional plane waves in a duct of arbitrary cross-section or circumferential modes in thin annular ducts. The network model of the CESAM-HP combustor is sketched in Fig. 2.

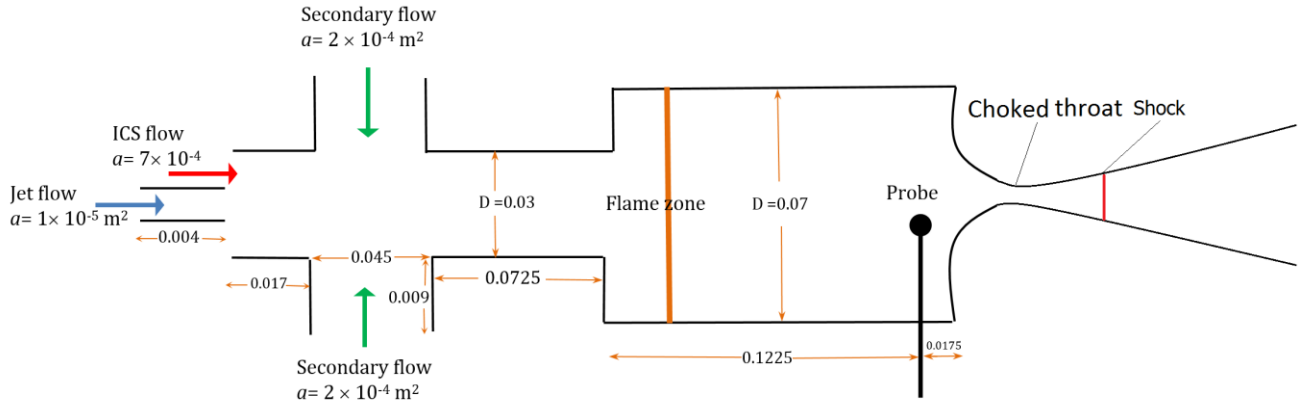


Figure 2: Schematic of CESAM-HP combustor used in LOTAN. All length dimension are in m.

For reductions in nozzle cross-sectional area and for gradual area increases, it is assumed that the mean flow does not separate so that isentropic conditions hold. Then, the mean flow quantities upstream and downstream of the area change are related to each other by applying conservation of mass, energy and angular momentum flow rates. The flame is modelled as a discontinuity on which the conservation of mass, momentum and energy flow rates are applied. It is a source in the energy flow rate equation which induces frequency-dependent acoustic and entropy fluctuations. The flame is placed between 0.01m and 0.02m in the combustor and the effect of flame positions on the Green's function is analysed. We assume that in the nozzle the region of supersonic flow between choked throat and the shock is compact, but the subsonic divergent and convergent sections are modelled as piece-wise isentropic area increases. The inlet of the short duct for air jet is taken to be acoustically non-reflecting. Flow in the ICS path is also taken to be a short duct with length of 0.004 m. The geometry of the perforated plate such as the number of holes, holes diameter, open-area ratio and their discharge coefficients are not known. Hence, we study the effect of different boundary conditions at the ICS inlet duct to be either non-reflecting or acoustically closed. As will be discussed in section 4.1 changing the boundary conditions at the inlet of the ICS duct has no noticeable effect on the pressure predicted in the combustor. The passage of the air and fuel in the secondary flow is modelled to be a short duct. The inlet of this short duct is connected to a large plenum. Combustor outlet is choked where the boundary condition of Marble and Candel [14] is applied. The nozzle then discharge burned gases to the atmosphere.

## 4. Results

In this section we first present the transfer function  $|\hat{p}/\hat{Q}|$  predicted by LOTAN for total, acoustic and entropy waves at the position of fourth microphone in Fig. 1 (i.e.  $x = 122.5$  mm from the combustor inlet). In LOTAN calculation to obtain the direct sound, we calculate the entropy wave generated at the flame but ignore their contribution when applying the downstream choked bounda-

ry condition. The direct sound field is obtained by adding the downstream and upstream propagating acoustic waves. The indirect noise due to the entropy wave can be determined by subtracting the direct noise from the full sound field calculated. Then using the spectrum of the heat release rate fluctuation, total, direct and indirect noise generated in the combustor is predicted and compared with experimental data. It should be pointed out that in the experiment and in high fidelity CFD it is very challenging to differentiate the contributions of direct and indirect noise sources. This challenging is mainly because measurements of the entropy fluctuations are very challenging.

#### 4.1 Effect of ICS inlet boundary condition on the transfer function (TF)

Figure 3 shows the amplitude of TF ( $|\hat{p}/\hat{Q}|$ ) for the total noise with two boundary conditions i.e. Non-reflecting and Closed at the inlet of the ICS path.

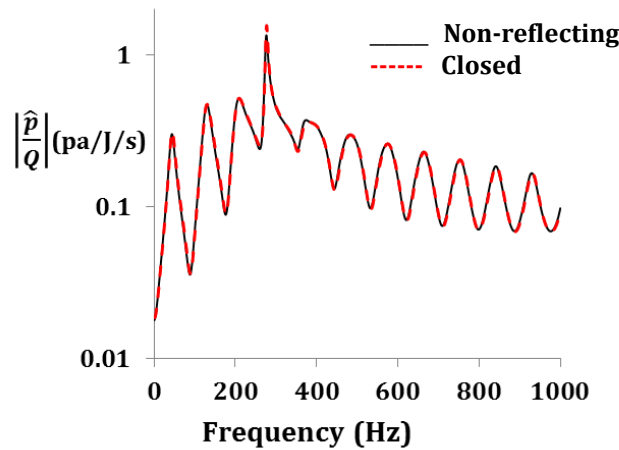


Figure 3: Amplitude of the transfer function for total noise as a function of frequency with two different boundary conditions at the inlet of the ICS, Non-reflecting (back solid line) and Closed (dashed red line).

The inlet of the jet duct is non-reflecting and that of the secondary duct is taken to be plenum. It is seen that utilising different boundary conditions at the ICS inlet has no noticeable effect on the TF predicted in the combustor. This is because the area in the secondary path is comparable to the main duct. Thus, plenum is like there being a large hole in the duct, and this decouples the acoustics at the upstream and downstream of this region. Thus, in the following we set the boundary condition at the inlet of the ICS to be non-reflecting.

#### 4.2 Effect of source position on the transfer function

When the heat release is so concentrated that  $\hat{G}_1(\vec{y}, \vec{x}, \omega)$  varies little over the combustion zone,  $\hat{G}_1(\vec{y}, \vec{x}, \omega)$  can be taken outside the source integral with respect to source position in Eq. (1).

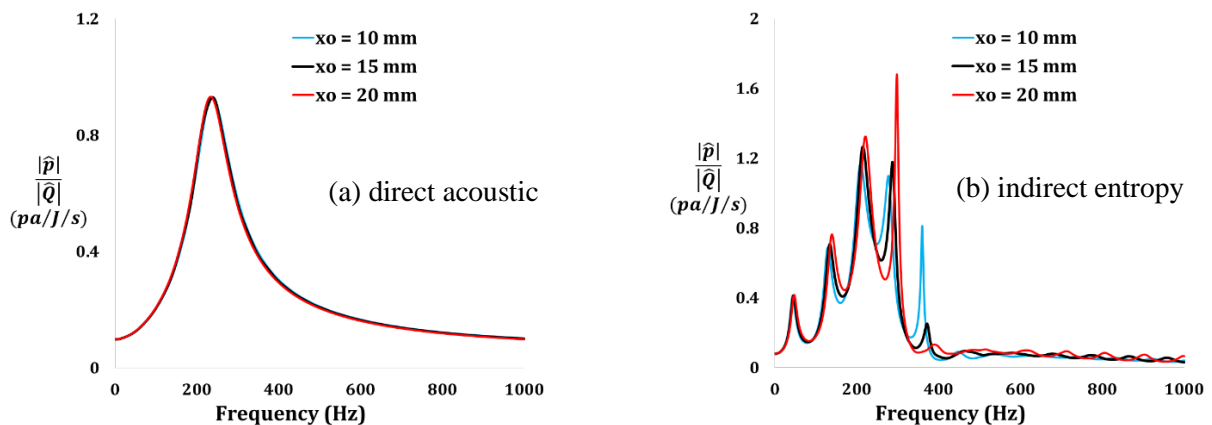


Figure 4: Amplitude of the transfer function for (a) acoustic noise and (b) entropy noise as a function of frequency with different source positions of  $x_0 = 10$  mm (blue line),  $x_0 = 15$  mm (black line) and  $x_0 = 20$  mm (red line) from inlet of the combustor.

Since the mean flow Mach number is low in the CESAM-HP combustor at the flame zone (i.e.  $\bar{M}_{\max} \approx 0.09$ ), it is a stronger constraint for the combustion zone to be short compared with the entropy wavelength  $2\pi\bar{u}/\omega$  than compared with the acoustic wavelength  $2\pi\bar{c}/\omega$ , where  $\bar{u}$  and  $\bar{c}$  are the mean axial velocity and speed of sound respectively. Here the effect of source position on the Green's function has been investigated. If the Green's function is strongly dependent on  $\vec{y}$ , one needs to run LOTAN for a number of axial source positions. According to the RANS simulation of the CESAM-HP combustor [5], most of the heat release occurs within the first 25% of the combustor length. We consider the variation of  $|\hat{G}_1|$  for a distribution of axial source positions within the first 25% of the combustor length at positions of  $x_0 = 10, 15$  and  $20$  mm. Transfer functions for acoustic and entropy waves are shown in Fig. 4. It is seen that the acoustic wave is not sensitive to the axial position for the whole range of frequencies considered. Thus, we are certain that if entropy waves are diffused before the fourth probe position,  $|\hat{G}_1|$  is not sensitive to the axial source position. Entropy wave shows slight dependency on the source position mainly at the peak frequencies. However, these peaks span over a very narrow-band of frequency range and hence their integral over frequency do not contribute significantly to the sound pressure level. Therefore, the results presented in Fig. 4 confirms that it is safe to take  $\hat{G}_1$  outside the source integral with respect to  $x_0$  and thus LOTAN needs to be run only once for each frequency.

### 4.3 The transfer function of combustion noise for the combustor

Figure 5 shows the amplitude of TF of total, direct and indirect noise as a function of frequency.

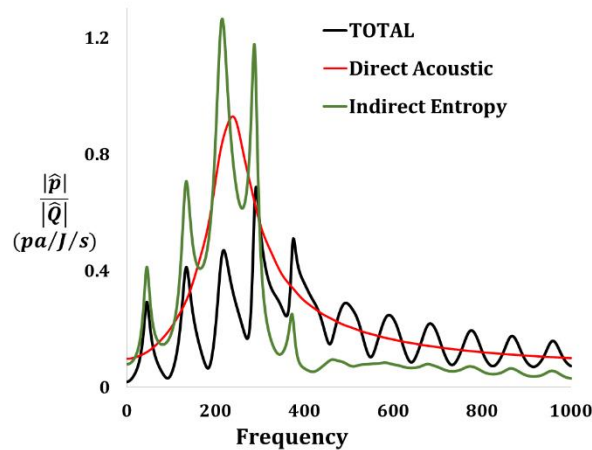


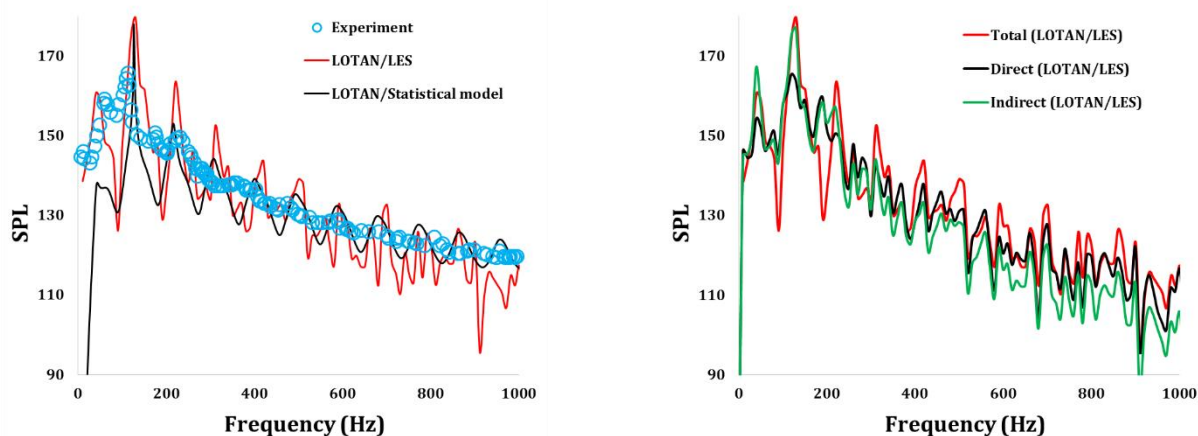
Figure 5: Amplitude of the transfer function for total (black line), direct acoustic (red line) and indirect entropy (green line) noise as a function of frequency.

It is seen that as the frequency tends to zero the TFs for total, acoustic and entropy noise tend to small values. As the frequency increase up to about  $f_{\text{peak}} = 250$  Hz (for acoustic and entropy noise) and  $f_{\text{peak}} = 300$  Hz (for total noise) the magnitudes of the pressure increase. Further increase in the frequency leads to decrease of the pressures generated. Indirect entropy noise has complicated dependency on the frequency. The shape of the total noise is mainly affected by the entropy noise and hence has multiple peaks and troughs. It is seen that for low frequencies below about 300 Hz the direct and indirect noise have similar magnitude and contribute similarly to the total noise generated in the combustor. For some frequencies the indirect noise is even higher than the direct acoustic

noise. For higher frequencies, the contribution of the entropy noise decreases but it is still high enough to contribute to the total noise generated.

#### 4.4 Sound pressure level

To predict the sound pressure level (SPL), the spectrum of the heat release rate fluctuation that is the source of direct and indirect entropy noise is obtained by two approaches, (i) by post-processing the compressible LES data of the CESAM-HP combustor [10], and (ii) using statistical noise model by Hirsch et al. [11]. The source obtained by these approaches is multiplied by the Greens' function for the total, acoustic and entropy noise predicted in section 4.3. Figure 6 (a) shows the total SPL predicted for the combustor utilizing these two noise sources into LOTAN, and their comparison with the experimental data. It is seen that the total noise predicted by LOTAN is in good agreement with the measured data and in-particular the frequency where the maximum SPL occurs,  $f_{\text{peak}} = 140$  Hz, is well-predicted. Nonetheless, the SPL predicted using statistical model for low frequencies is under predicted. Because as explained in [5] the maximum amplitude of the integral heat release spectra at the peak frequency, as well as the slope of the spectrum are highly under-predicted compared to the LES data. The Hirsch et al. [11] spectral model requires mean flow and turbulent properties such as, velocity, density, turbulent intensity, turbulent dissipation and etc.



(a) SPL as a function of frequency for total predicted noise using LOTAN in combination with LES (red line), and statistical model (black line) compared with the measured data [10] (symbols).

(b) Predicted Sound Pressure Level as a function of frequency for total noise (black line), direct acoustic (red line), indirect entropy (green line) based on heat release spectrum obtained using LES data [10].

Figure 6: Sound Pressure Level as a function of frequency.

It was shown in [5] that RANS cannot well-predict the flow properties of the CESAM-HP combustor. Consequently the heat release spectrum and the SPL are not well-predicted. Figure 6(b) demonstrates the contribution of direct acoustic and indirect entropy noise to the total noise generated in the CESAM-HP combustor. It is seen that the indirect entropy noise and direct acoustic noise contribute similarly to the total noise generated. Nonetheless, at frequencies above  $f_{\text{peak}}$  the contribution of the direct acoustic noise is slightly higher. Recent work by Huet et al. [10] concluded that the total noise reflected by the nozzle in the combustor is predominant by the direct contribution. Nonetheless, in the paper they discussed that their predicted direct acoustic noise includes the multiple reflection of entropy-generated noise by the combustor boundaries. Thus, in their analysis the direct and indirect noise counterparts were not fully differentiated.

## 5. Conclusions

Low order model (LOTAN code) in combination with spectrum of the heat release rate fluctuation has been used to predict the broadband combustion noise and its direct and indirect contribu-



tions in the lab-scale CESAM-HP combustor. Two approaches have been utilised to determine the spectrum of the heat release rate fluctuation for an unsteady turbulent partially premixed flame. In the first approach, results of LES have been post-processed to calculate the spectrum of heat release rate fluctuation. In the second approach, spectral model developed by Hirsch et al. [11] and modified by Liu et al. [12] based on RANS data, has been used to obtain the spectrum of heat release rate fluctuations. The spectrum then combined with the Greens' function predicted by LOTAN to obtain the spectrum of broadband combustion noise in the combustor. The total noise predicted utilising LES spectrum agrees well with the measured data. Contribution of direct and indirect noise in generation of total noise at the combustor outlet is identified. It was found that for frequencies below  $f_{\text{peak}}$ , the indirect entropy noise has comparable contribution to the direct acoustic noise in the generation of total noise. While for frequencies above  $f_{\text{peak}}$ , the contribution of the indirect entropy noise is modest. Results also showed that for the second approach utilising the statistical model using RANS data and for frequencies below 250 Hz, the combustion noise is under-predicted by 20 dB. But, for higher frequencies the predicted noise were in good agreement with experimental data.

## 6. Acknowledgements

This work was funded by the European Commission part of the RECORD (Research on Core Noise Reduction) project under Grant No. RG66913.

## REFERENCES

- 1 Dowling, A. P. and Mahmoudi, Y. Combustion noise, *Proceedings of the Combustion Institute*, **35**, 65–100, (2015).
- 2 Cumpsty, N. A. Jet Engine Combustion Noise: Pressure, Entropy and Vorticity Perturbations Produced by Unsteady Combustion or Heat Addition *Journal of Sound and Vibration*, **66**, 527-544, (1979).
- 3 Kings, N., Tao, W., Scoufnaire, P., Richecoeur, F., Ducruix, S. Experimental and numerical investigation of direct and indirect combustion noise contributions in a lean premixed laboratory swirled combustor, *ASME Turbo Expo 2016: Turbomachinery Technical Conference and Exposition* (pp. V04BT04A047-V04BT04A047), *American Society of Mechanical Engineers* (2016).
- 4 Livebardon, T., Moreau, S., Poinot, T., Bouty, E. Numerical investigation of combustion noise generation in a full annular combustion chamber, *21<sup>th</sup> AIAA/CEAS Aeroacoustics Conference*, (p. 2971), (2015).
- 5 Ulrich, W. C., Hirsch, C., Sattelmayer, T., Mahmoudi, Y., Dowling, A. P., Swaminathan, N., Lackhove, K., Sadiki, A., Fischer, A., Stauffer, M. Prediction of combustion noise in a model combustor using a network and a LNSE approach, *ASME Turbo Expo 2017: Turbomachinery Technical Conference and Exposition (GT2017)*. *American Society of Mechanical Engineers, Charlotte, United States, 26-28 June*, (2017).
- 6 Mahmoudi, Y., Dowling, A. P., Stow, S. Direct and Indirect Combustion Noise in an Idealised Combustor, *25<sup>th</sup> Int. Colloquium on the Dynamics of Explosions and Reactive Systems (ICDERS)*, Leeds, UK, (2015).
- 7 Mahmoudi, Y., Dowling, A. P., Stow, S. Acoustic and entropy waves in nozzles in combustion noise framework, *AIAA Journal*, (Accepted), (2017).
- 8 Mahmoudi, Y., Giusti, A., Mastorakos, E., Dowling, A. P. Low-order modelling of combustion noise in an aero-engine: the effect of entropy dispersion, *ASME Turbo Expo 2017: Turbomachinery Technical Conference and Exposition (GT2017): Proceedings, Charlotte, United States, 26-28 June*, (2017).
- 9 Stow, S., Dowling, A. P. A time-domain network model for nonlinear thermoacoustic oscillations, *ASME Transactions, Journal of Engineering for Gas Turbines and Power*, **131**(3), (2009).

- 10 Huet, M., Vuillot, F., Bertier, N., Mazur, M., Kings, N., Tao, W., Scouflaire, P., Richecoeur, F., Ducruix, S., Lapeyre, C., Poinso, T. Recent Improvements in Combustion Noise Investigation: from the Combustion Chamber to Nozzle Flow, *AerospaceLab*, (11), 10, (2016).
- 11 Hirsch, C., Wasle, J., Winkler, A., Sattelmayer, T. A spectral model for the sound pressure from turbulent premixed combustion. *Proceedings of the Combustion Institute*, **31**, 1435–1441, (2007).
- 12 Liu, Y., Dowling, A. P., Swaminathan, N., Morvant, R., Macquisten, M. A., Caracciolo, L. F. Prediction of combustion noise for an aeroengine combustor, *Journal of Propulsion and Power*, 30(1), 114-122, (2013).
- 13 Mazur, M., Tao, W., Scouflaire, P., Richecoeur, F. and Ducruix, S. Experimental and Analytical Study of the Acoustic Properties of a Gas Turbine Model Combustor With a Choked Nozzle, *ASME Turbo Expo 2015: Turbine Technical Conference and Exposition* (pp. V04BT04A001-V04BT04A001). *American Society of Mechanical Engineers*, June, (2015).
- 14 Marble, F.E., and Candel, S. Acoustic disturbances from gas nonuniformities convected through a nozzle, *Journal of Sound and Vibration*, **55**, 225–243 (1977).